Including spatially variable precipitation and temperatures in the the Shallow Ice Approximation (SIA) model for Antarctic ice thickness estimates

Kelian Dascher-Cousineau

December 26, 2016

1 Introduction

The future of the Antarctic Ice Sheat (AIS) is a contentious subject matter [7]. Its future is tightly tied into global sea levels and climate, thus having substantive societal impacts [1]. In the context of today's aggressive anthropogenic climactic forcing, expressed in elevated global temperatures, sea levels, modelling is one of the few tool we have to predict the behaviour of the AIS both in the short and long term [1].

Ice sheet models vary in complexity, applicability, practicality and validity. Choosing an appropriate model is strongly dependent on the on the physical context of study, time window of interest, available computational resources, parameters uncertainties and, ultimately, the research question that is set out to be answered. In the study of ice sheets, most current models describing long term deformation derive either entirely, or in part, from physical descriptions of fluid flow [8]. Notwithstanding superficial brittle features such as fissures and crevasses, ice sheets most readily deform by viscous flow [12]. In the study of continental scale ice flow, the *Shallow Ice Approximation* (SIA) has been a widely used model. Its popularity is broadly attributable to is computational simplicity [9]. While the SIA also derives from computationally complex formulations of fluid flow, it owes its simplicity to simplified rheological laws, spatially invariable conditions and, most importantly, dropped stress terms, negligible when bed slopes and velocity gradients are small [9].

In this short study, I adapt an explicit model formulation of the SIA to incorporate the effect of variable temperature and ice pressure on the surface mass balance and on the fluidity of the ice. The general intent is to explore the long term ($> 10^3$ years) sensitivity of the AIS to temperature changes. Specifically, I exact the sensitivity of steady state conditions, and the corresponding stabilization rate. To do so, I build upon a working SIA model written in the *MatLab* scripting language. In this report, I first test my adapted model with benchmarks, computational sensitivity tests and robustness tests. I then explore a range of physically realistic temperature trends and their respective effect on the stability, sustainability and general evolution of the AIS.

2 Model Outline

2.1 The Shallow Ice Approximation

The *Shallow Ice Approximation* (SIA) is a simplification of the Navier-Stokes viscous flow equation for a slow, incompressible flow on a shallow slope with a fixed, zero velocity, basal boundary condition. In this section, I derive the shallow ice approximation and discuss both its limitations and advantages. The general intent of this section is to elucidate the physics of continental scale ice flow and the computational methods that can be used to describe them. Note that the outline of the SIA presented here follow the structure Bueler's course notes.

The *Navier-Stokes* states that fluid flow must respect:

$$\nabla \cdot \mathbf{u} = 0, \tag{1}$$

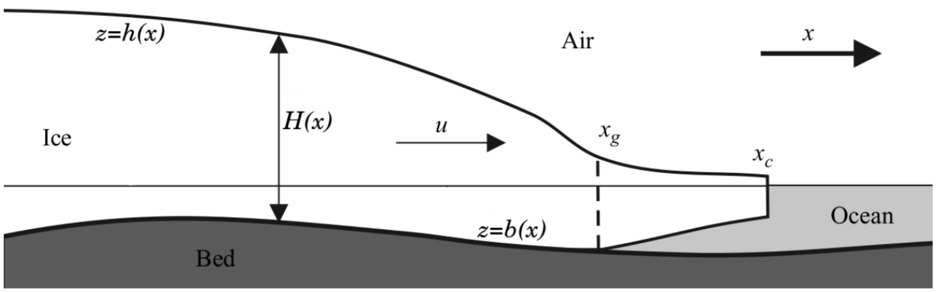

Figure 1: Schematic outline of the SIA model cross sectional view of a flowing glacier. x, y (not shown) and z are the horizontal and vertical dimensions respectively, $h(x, y)$ is the surface elevations of the ice sheet, $b(x, y)$ is the bed topography, $H(x, y) = h - b$, is the thickness of the ice sheet, u is the velocity of the ice sheet, x_g is the grounding line and x_c is the calving front.

where $\mathbf{u}$ is velocity, to describe the incompressibilty of fluids; and

$$\rho(\mathbf{u}_t + \mathbf{u} \cdot \nabla \mathbf{u} = -\nabla p + \nabla \cdot (\nu \nabla \mathbf{u}) + \rho g, \tag{2}$$

where rho is density, p is pressure, ν is viscosity and g is the gravitational acceleration, to describe the stress balance of the fluid flow. Note that the derivations of the incompressibility and Navier-Stokes equations is nicely outlined in Gerya, 2009 [6]. The left hand side of the stress balance equation effectively represents the acceleration of the fluid. In the case of ice flow, acceleration terms become negligible and can be dropped so that the *slow flow* can be described as follows:

$$\nabla \cdot \mathbf{u} = 0, \tag{3}$$

$$0 = -\nabla p + \nabla \cdot (\nu \nabla \mathbf{u}) + \rho g \tag{4}$$

The rheology of ice is not linear. As a result, viscosity ν is not constant. The $(\nu \nabla \mathbf{u})$ is rather expressed according to the shear stress tensor, τ_{ij} which is constrained by empirical flow laws. The $n = 3$ *Glen flow law* is commonly used when describing ice flow:

$$Du_{ij} = A\tau^2 \tau_{ij} \tag{5}$$

where u_{ij} is the strain tensor, A is an empirical scaling constant.

Consider the 2 dimensional (in the x and z cross section) plane flow rotated into the frame of reference of the slope (by angle $alpha$) of a slab of ice of thickness H. Equations 3, 4 and 5 simplify to:

$$w_z = 0 \tag{6}$$

$$\tau_{13,x} = -\rho g \sin \alpha \tag{7}$$

$$p_x = -\rho g \cos \alpha \tag{8}$$

$$0 = \tau_{11} \tag{9}$$

$$u_x = 2A\tau^2 \tau_{13} \tag{10}$$

where u and w is the velocity in the x and z direction respectively. Subscripts indicated derivative operations. Given the boundary conditions:

$$w(0) = 0, \tag{11}$$

$$p(H) = 0, \tag{12}$$

$$u(0) = u_0, \tag{13}$$

the analytical solution,

$$u = u_0 + \frac{1}{2} A(\rho g \sin \alpha)^3 (H^4 - (H - z)^4) \tag{14}$$

describes the flow of the slab as a function of depth.

We wish to describe the deformation of ice *over time*. The temporal variation is captured in the continuity equation:

$$H_t = M - (\bar{u}_1 H)_x \tag{15}$$

where H_t is the time derivative of the thickness of the ice sheet, M is the surface mass balance, and $\bar{u}$ is the mean velocity, vertically integrated, of the flow:

$$\bar{u} = \frac{1}{H}\int_0^H u dz. \tag{16}$$

Combining equations 14, 15, 16, setting the basal flow velocity to zero, and approximating $\sin\alpha \approx \tan\alpha = -h_x$ (small angle approximation, we obtain the SIA

$$H_t = M + \left(\frac{2}{5}(\rho g)^3 A H^5 |h_x|^2 h_x\right)_x. \tag{17}$$

Generalized to two horizontal directions, the slab flow becomes

$$\mathbf{U} = \frac{2A(\rho g)^n}{n+1}[H^{n+1} - (h-z)^{n+1}]|\nabla h|^{n-1}\nabla h, \tag{18}$$

Mass continuity becomes

$$H_t = M - \nabla \cdot (\bar{\mathbf{U}} H), \tag{19}$$

which in turn yields the 2D SIA:

$$H_t = M + \nabla \cdot (\Gamma H^{n+2} |\nabla h|^{n-1} \nabla h) \tag{20}$$

where $\Gamma = 2A(\rho g)^n/(n+2)$.

Note that while this derivation was based on a slab of equal thickness on a constant slope, the approximation is generalizable to variable slopes and thickness if the spatial gradients are small. In the context of continental scale ice flow this approximation is valid. Here, average topographic gradients are small, and spatial variability of the thickness of the AIS is very gradual.

2.2 Numerical Implementation of the SIA

No analytical solution can be derived to capture the temporal in ice thickness prescribed by the SIA. We must therefore revert to numerical schemes to approximate the its solution. In doing so, it is first important to note that the SIA is *diffusive*; in the same way heat diffuses away from a heat source, the AIS is diffusing away from points of precipitation. This correspondence is also expressed in their respective governing equations:

SIA (H is ice thickness)	heat: T is temmperature
$H_t = M + \nabla \cdot (\Gamma H^{n+2} \vert\nabla h\vert^{n-1} \nabla h)$	$T_t = F + \nabla \cdot (D\nabla T)$

Here we see that, according to the SIA, the 'diffusivity' (D) of a glacier is:

$$D = \nabla \cdot (\Gamma H^{n+2} |\nabla h|^{n-1}) \tag{21}$$

This observation is going to guide the approach by which the SIA will be solved. Consider the 'shifted' diffusion equation:

$$T_t = F + \nabla \cdot (D\nabla(T + b)). \tag{22}$$

This equation can be approximated on a regularly spaced spacial grid with J by K nodes at N regular time intervals in according to the following finite difference scheme on a stagerred grid:

$$\begin{aligned}\nabla \cdot (D\nabla X) \approx\ & \frac{D_{j+1/2,k}(X_{j+1,k} - X_{j,k}) - D_{j-1/2,k}(X_{j,k} - X_{j-1,k})}{\Delta x^2} \\ & + \frac{D_{j,k+1/2}(X_{j,k+1} - X_{j,k}) - D_{j,k-1/2}(X_{j,k} - X_{j,k-1})}{\Delta y^2}\end{aligned} \tag{23}$$

X is the temperature and could simply be denoted as T. In its formulation, it does however also allow for a 'shift' (i.e. $X = T - b$), one that will be useful in for the implementation of the SIA with variable bedrock topography. The staggered grid ensure better numerical stability by essentially simplifying the parameter approximation at neighbouring nodes. The physical state (T^{n+1}) at the following time step is solved for *explicitly* by simply multiplying either side of the equation by the time increment. Therefore, given an initial state, T_0, a diffusivity, D and a spatial 'shift', b, the projected physical state can be estimated on the spatial grid iteratively using the numerical approximation outlined above. The choice of for time steps is done according to an adaptive time-stepping scheme. This prevents the model from becoming unstable by ensuring the proper averaging across the numerical stencil.

The explicit solution to the SIA builds upon this diffusion scheme. To do so, the diffusivity, D of the ice cap and the thickness of the ice cap (with the added surface mass flux) is calculated externally after every time step. These are then imputed into the diffusion scheme. The diffusion scheme is allowed run for a specified time increment (the incrementation of the overall SIA model).

2.3 Adapting the SIA

In this study, I incorporate functionality for spatially variable temperature. The module is built so as to adapt the isothermal SIA model. Temperature affects SMB and rheology. This module basically functions by querying temperature conditions at each node on the horizontal grid and adapting rheological and SMB parameters accordingly. The temperature is obtained on the basis of its correlation with topography. The following two section present, in more detail, how the this effect is measured and incorporated, numerically, into the SIA model.

2.3.1 Effect on rheology

As mentionned above, the rheology of ice is described by a glen flow law:

$$Du_{ij} = A\tau^2\tau_{ij} \tag{24}$$

The terms $A\tau^2$ represent the fluidity of the ice. A strong temperature dependence for the rate factor, A, is made evident in its expansion, the *Arrhenius law*:

$$A(T,p) = A_0 e^{-(Q+pV)/RT}, \tag{25}$$

where A_0 is the pre-exponent constant, Q is the activations energy, V is the activation volume, R is the universal gas constant, T is the temperature and p is the pressure. Experiments show that simplifying the Arrhenius law to:

$$A(T') = A_0 e^{-Q/RT'}, \tag{26}$$

where $T' = T - T_m = T + \beta p$ is the temperature relative to the pressure melting point. Typical values for the parameters of the Arrhenius law are presented in table 1. It should become clear that the fluidity of ice should highly sensitive to temperature changes since the temperature dependence is embeded in the exponent of the Arrhenius law.

What values of temperature and pressures are used? These are both subject to change with depth which complicate the SIA model derivation. For the purpose of simplicity and tractability, the implementation presented here does not take into account the variability with depth. Instead, a representative temperature and pressure is taken at the half depth of the AIS assuming a linear temperature and pressure profile with gradients G and $\rho_{ice}g$ respectively (also included in table 1). These P-T conditions are then used to obtain the representative fluidity on the horizontal grid. The full implementation of variable temperature is superficially explored in the discussion section.

At each time block the thickness of the ice sheet is updated. Accordingly, the surface elevation changes, the representative pressure and temperature change and, in turn, the fluidity changes at every point on the computational grid. The implementation of this module involved:

- the creation of a *fluidity* function;

Parameters	Value	
Per-exponential constant, A_0	$3.985 \times 10^{-13} s^{-}1 Pa^{-3}$	(for $T' \leqslant 263.15K$)
	$1.916 \times 10^{3} s^{-1} Pa^{-3}$	(for $T' \geqslant 263.15K$)
Activation energy, Q	$60 kJmol^{-1}$	(for $T' \leqslant 263.15K$)
	$139 kJmol^{-1}$	(for $T' \geqslant 263.15K$)
Clausius-Clapeyron constant, β	$9.8 \times 10^{-8} KPa^{-1}$	(for water saturate Ice)
Temperature gradient, G	$\approx 0.01 Km^{-1}$	(for steady state diffusion)
Pressure gradient, ρg	$910.0 kg/m^3 \times 9.807 ms^2$	

Table 1: Parameters for the Arrhenius law [12]

.

- creating temperature and fluidity grids;
- incorporating element-wise multiplication throughout the model;
- incorporating the variable fluidity in the stencil of the SIA model.

2.3.2 Effect on surface mass balance

In this model, I take the rather rudimentary approach to simply use existing correlations between temperature and precipitation. The actual interplay between temperature and SMB is a lot more complicated.

Given simple linear correlations in the 10^3 year time scale. I incrementally change the accumulation rate based on the correspond change in temperature. This change is again implemented by updating the SMB after every time block given evolving global temperatures and, changes in temperature driven by surface topography changes.

2.4 Data

The following four spatial datasets of the AIS are combined in this study: 1) bed rock elevation, 2) ice surface topography, 3) temperature/topography correlation and 4) surface mass flux/temperature correlation. The former two datasets are included within Buelers original code. These are sourced from In this section, I briefly discuss the sources of these datasets along with the general methods used to acquire them.

2.4.1 Temperature

In this study, temperature is not acquired directly. Instead, the approach presented here is based on a strong correlation between ice surface elevation and temperature. For reference, figure 2 is the aggregation of temperature measurements of ice cores at 10 m of depth from the THERMAP: Ice Temperature Measurements of the Antarctic Ice sheet database [3]. At 10 m of depth, seasonal variations in temperature are attenuated. These temperature measurements therefore serve as a robust measurement of mean annual temperatures. While these temperature measurements are not particularly recent, there values should be satifactory on the time scale that is modelled, that is for time increments upwards of hundreds of years.

2.4.2 Surface Mass balance (SMB)

Surface mass balance acts as a forcing agent in the SIA model. The specific SMB is defined by the precipitation (P), surface sublimaiton (SU_s), run of due to melt (RU) and erosion by ($ER_d s$) and sublimation of snow drifting ($SU_d s$) such that:

$$SSMB = \int_{year} (P - SU_s - RU - ER_{ds} - SU_{ds}) dt \tag{27}$$

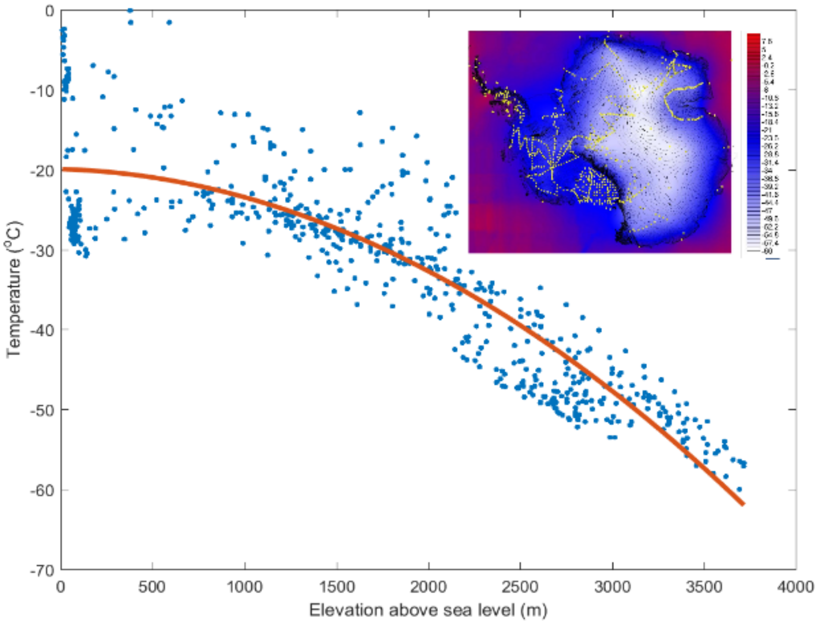

Figure 2: Left: Relationship between 10 m core temperatures and elevation above sea level on the Antarctic ice shelf. Fifth order polynomial is fit to this data. This correlation is used in model to query spatially variable temperature. Right: Map of the AIS with locations of the 10 m core data (yellow points) and interpolated temperature color map

All these factor are subject to strong spatial variations. The distribution of which is still subject of active dicussion in the litterature. Direct measurements of SMB are not readily available are the continental scale. For the purpose of simplicity, I rather use a correlative approach based on empirical relationships for the AIS. Incremental correlations are typically around $0.06/^oC$ [5, 4]. This correlation is nevertheless variable depending on the time window of study and also spatially variable [5].

3 Model testing

In this section, I outline the steps taken to ensure that the adapted model is not embedded with mistakes. These principally include buds and numerical instabilities.The code is laced with small changes to allow for spatially variable temperatures and fluidity parameters, a first screening test was to benchmarked to its original counterpart. Bueler's original code is benchmarked to analytical solution; tested for sensitivity to both grid size and time steps; and tested for robustness. A test against Bueler's codes ensures that the changes did not affect the original functionality.

Subsequent test presented hereafter are built upon from the AIS set up. At this point the main concern to pick potential errors and establish the numerical domain of stability.

3.1 Sensitivity

The cumulative ice volume, the numerically integrated AIS thickness, is tracked over time each time iteration. The temporal evolution of this volume is used to test the sensitivity of the model. Specifically, the effect of varying time increment size is tested. This is shown in figure 3 for spatially variable temperature unchanged over time. All models, converge towards the same steady state solution. Models with time increments more than 10 time increments are nearly indistinguishable. The exception to this being the short term response (100 years) which differ in the progressively finer models. However, the early spike is likely due to unrealistic edge effects associated to the calving of the ice sheet.

The model is expected to have little sensitivity to the time incrementation. This is because the *newdiffusion* function, at the core of the model, self-defines time increments so as to stay stable.

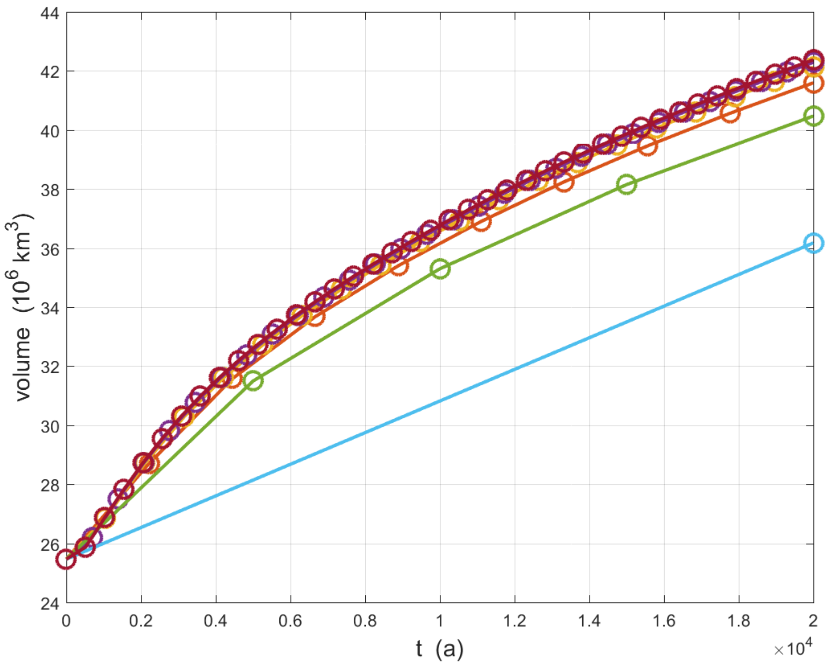

Figure 3: Sensitivity to time incrementation over the time frame of $20ka$. The time domaine was iteratively divided into 2 (blue), 5 (green), 10 (orange), 20 (yellow), 30 (purple) and 40 (red) increments of time.

Moreover, the *siageneral* function does not change its time incrementation (it remains constant at 1 year). The sensitivity that we *do* observe is associated to updating calving fronts and fluidity values after each time blocks.

3.2 Robustness

Robustness namely tests, in a qualitative sense, the stability of the code to extreme initial conditions. These will likely break some of the implicit assumption of the SIA, thus yielding physically unrealistic results, they provide qualitative check for the ability of the code to function under more extreme conditions. Positive results here are first order indications that the AIS is 'diffusing'. To test the robustness of the adapted SIA, the initial topography is doubled. Figure 4 shows the robustness to a randomized and amplified initial ice topography. Note that the randomized ice topography has the implicit effect of changing the temperature field (correlated to absolute elevation above sea level). The model was also tested under more extreme model conditions (i.e. thicker initial ice bed). The model slows down to a crawl at these conditions. This limitation is not a shortcoming to the numerical method but rather of the physics of the problem. Increasing the thickness of the bed has multiple effects. 1) It increases the driving stresses of the system. 2) It changes the surface topography height which in turn changes the surface temperature. 3) It increases the isolating capacity of the glacier. The latter two effects have important repercussions in the numerics of the model. In fact, the temperature used to calculate ice fluidity is systematically higher because insulating effect is stronger than the topographic effect. Increased temperature drives the fluidity of the system up and in turn requires finer temporal resolution. In attempt to compensate for this the adaptive stepping in the *newdiffusion* function decreases to unpractically small time increments. In short, the model is not robust, but only to physically unrealistic conditions. In the study context, this should not be an issue.

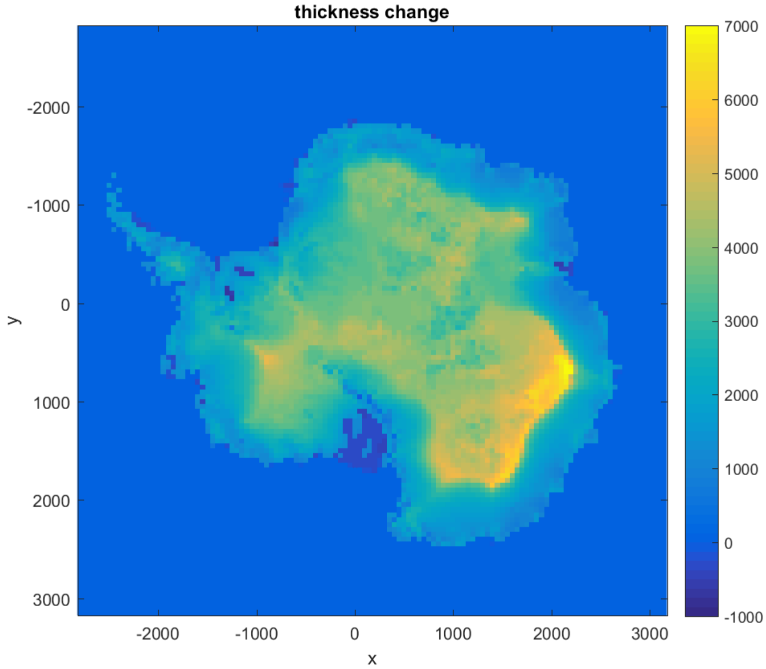

Figure 4: Thickness change over 20000 years using spatially variable temperature but consistent over time. Ice thickness is doubled to test the robustness of the model. x and y axes are in kilometers with thickness change (colorbar) in meters.

4 Results

The first order result of this study is the addition of spatially variable temperature and, in accordance, spatially variable fluidity. Figure 5 shows how this changes the AIS thickness. Here, we see a general trend of increasing AIS thicknes, with a few exptions on coastal areas near the grounding line. The center of the AIS shows a less intense increase increase in thickness.

Now, I increase the model complexity by adding an increasing temperature trend. The temperature trend is set to 20 degrees Celsius over the 2000 year domain. In this run, SMB is still unchanged over time. Figure 6 shows the change in glacier thickness after 2000 years. The final differential picture is very different to that of the default set up when temperature remains unchanged. While it is again the case the the AIS is generally increasing in thickness (with the exception of points in proximity to grounding lines, the increase in thicknes is much more subdued. To further explore the sensitivity of the AIS to temperature induced changes in fluidity, I test a range of warming rates and track the total volume of ice over time (see figure 7).

I now also include the the temperature induced changes in SMB. Figures 8 and 9 show the added effect of evolving SMB. In doing so, I find that there is little difference to the latter scenario.

5 Discussion

The adapted SIA model yields some predictable results. As the AIS is perturbed it "diffuses" away from areas with high precipitation. Diffusion beyond the calving front is removed from the system as would be predicted. When the system is not continually forced, the AIS tends towards a steady state condition–a state when the calving rate essentially balances out the positive SMB. On the other hand, when the model is clearly highly sensitive to temperature changes. This is accordant with the exponential temperature term in the Arhennius law which defines the fluidity of the ice. Increasing the fluidity allows for more effective flow of the ice sheet off the continent towards the calving fronts. It is interesting (and somewhat alarming) to note that while the temperature forcing presented in this study may appear overly aggressive (up to ^{o}C over the 20000 year period) it is still more than an order

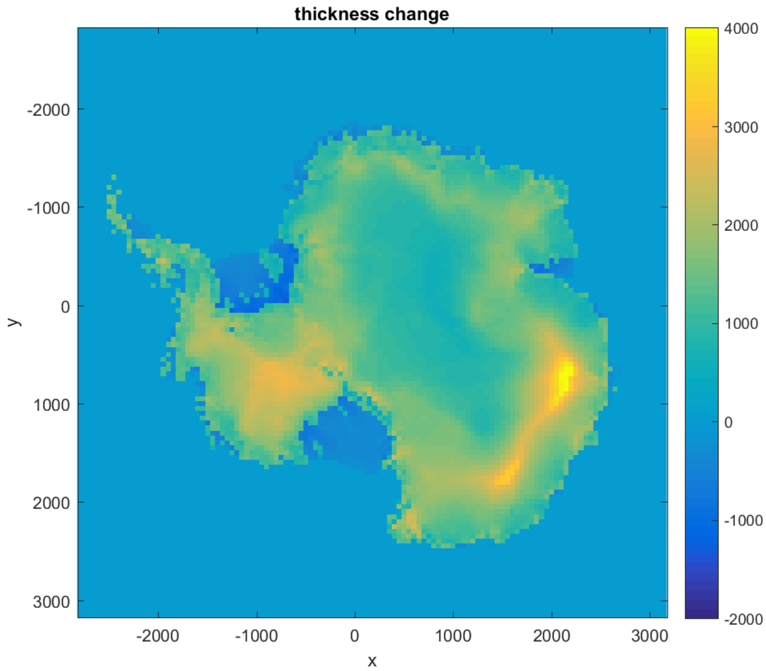

Figure 5: Thickness change over 20000 years using spatially variable, but temporally constant, temperature and SMB. Temperature is forced at a rate of 20 celcius over the 20000 year time window. x and y axes are in kilometers with thickness change (colorbar) in meters.

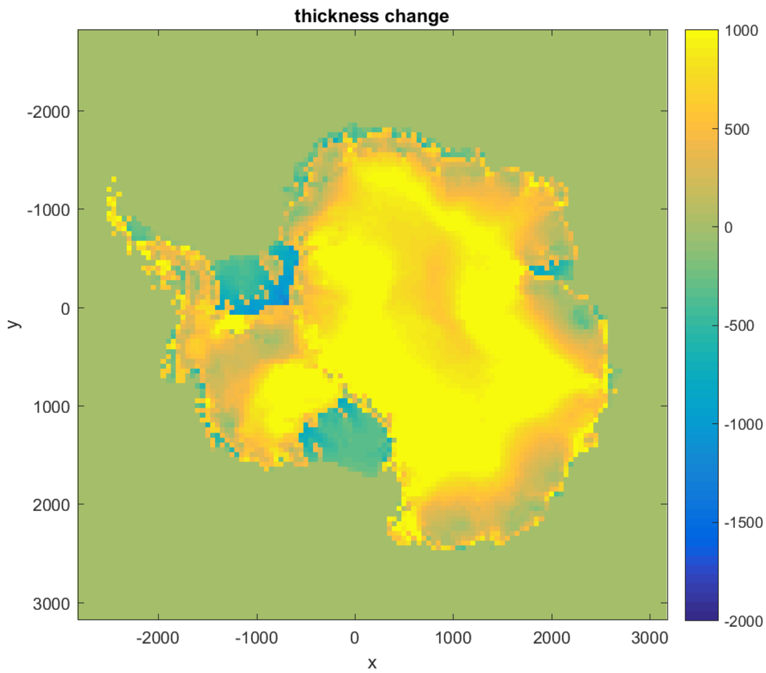

Figure 6: Thickness change over 20000 years using spatially variable and increasingly hotter temperature. For this result, SMB is held constant. x and y axes are in kilometers with thickness change (colorbar) in meters.

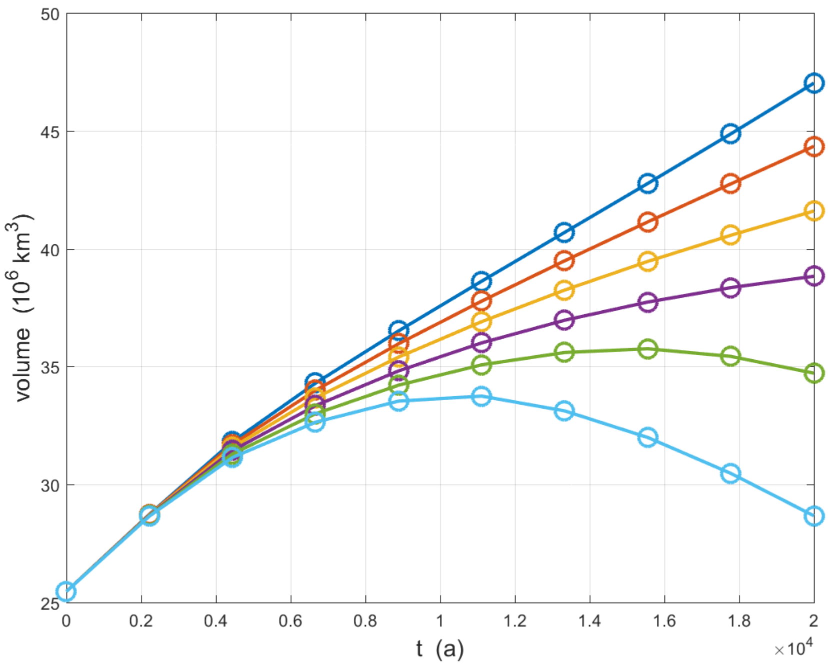

Figure 7: Volume of the AIS as a function of time for a range of cooling to warming rates with the SMB held constant. From top to bottom the rates range from -20 to +40 ^oC change in temperature in the 20000 year time window (in increments of 10 ^oC).

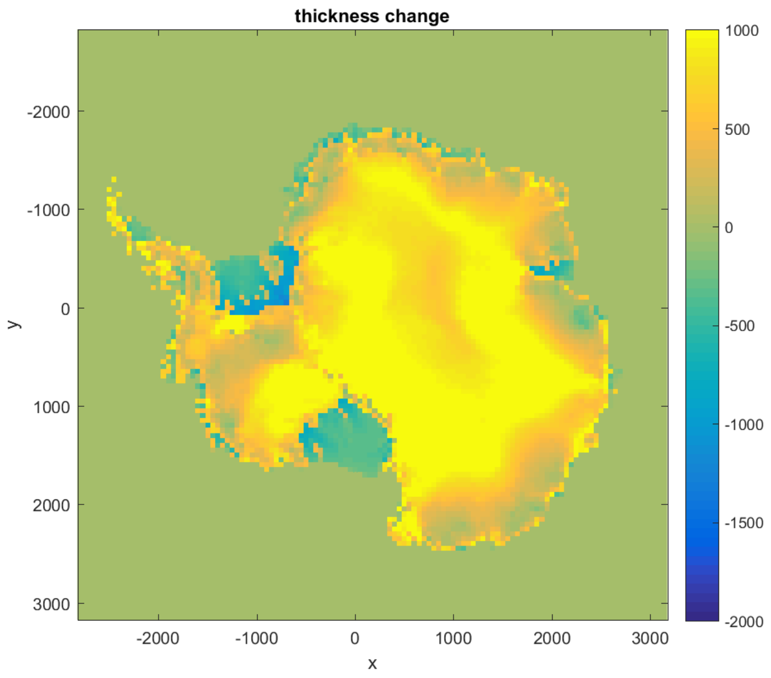

Figure 8: Thickness change over 20000 years using spatially variable and increasingly hotter temperature. For this result, SMB is also increased by 6 percent for every degree increase in temperature. x and y axes are in kilometers with thickness change (colorbar) in meters.

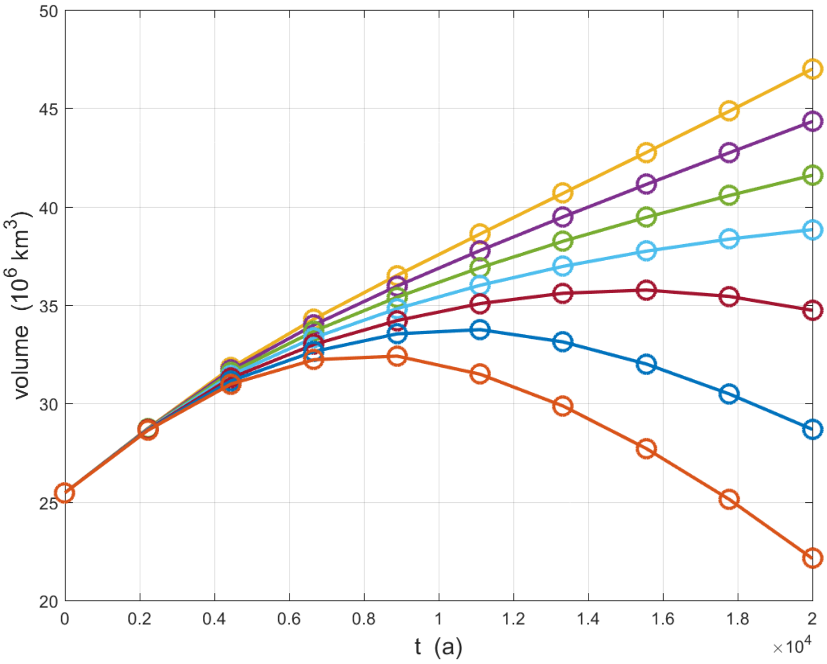

Figure 9: Volume of the AIS as a function of time for a range of cooling to warming rates with the SMB held constant. From top to bottom the rates range from -20 to +40 ^oC change in temperature in the 20000 year time window (in increments of 10 ^oC).

of magnitude less than the trend of the last 100 years [10]. Conversely, the increased precipitations induced by the increased temperature has, as one would expect, the converse effect of stabilizing the AIS total volume. However, the effect of the increased precipitation, under realistic temperature/precipitation correlation, appears to be substantial enough to make a significant difference in comparison to the temperature induced change in ice fluidity. This is consistent with an exponential relation (temperature/fluidity) overshadowing a linear relationship (temperature/precipitation).

On the other hand, there are, *a priori*, unexpected features of the model. The general trend of *increasing* in volume is, to a first order interpretation, unexpected, especially considering that it is known according to gravimetry [13] and state of the art models [7] that the AIS volume is decreasing. Ideally, the default model with the temperature held fixed over time would remain in a steady state since it is not intentionally being excited in the first place; the conditions were chosen to replicate those of the current AIS. This points to the fact that the model is presenting an incomplete description of the AIS physics. Specifically, the model is either not capturing mechanisms by which the AIS can remove ice or over estimating the SMB (or, likely, both). This is not entirely surprising since the SIA entirely omits mechanisms by which ice can flow faster, this includes but is not limited to, basal sliding, brittle deformation, and further increases in fluidity down the vertical temperature profile.

In this study, I only included variability in temperature in horizontal dimension. While this is an improvement on the the isothermal model, it is important to note that a more complete incorporation of variable temperature should explore changes with depth. Indeed, the typical vertical temperature profile is not not constant. Its inclusion in the SIA does, however, greatly complicate the derivation of the model. Equation 14, presented the solution to:

$$u_z = 2A(-\rho g \sin\alpha)^3 (H-z)^3 \tag{28}$$

The rate coefficient, A, defined by the Arrhenius law, *does* depend on pressure and the vertical temperature profile. The integration is complicated and no longer can no longer be described by a tractable analytical solution. It may however be possible to expand the Arrhenius law and its variability with depth:

$$A(z) = A_0 e^{Q/RT'(z)} \tag{29}$$

where $T' = T(z) - \beta p(z)$, into a Taylor series, thus making the integration tractable. While the integration would not yield a particularly compact result, the continuation of the derivation of the SIA model would not be affected by the additional polynomial terms. The accuracy of the model would however be sensitive to the order of truncation. For the purpose of explanation, I present the simplest 'first order' model. Assuming a linear vertical temperature profile with surface temperature T_0 and temperature gradient G, equation 29 becomes:

$$A(z) = A_0 e^{Q/R(T_0 - z(G-\rho g))} \tag{30}$$

and represented, near $z = 0$ as a series according to

$$\begin{aligned} A(z) &= A_0 \left(e^{Q/RT_0} + \frac{Q(G-\rho g)xe^{Q/RT_0}}{RT_0^2} + \frac{Q^2(G-\rho g)^2 x^2 (Q/R + 2T_0)e^{Q/RT_0}}{2R^2T_0^4} + ... \right) \\ &\approx az + b \end{aligned} \tag{31}$$

where

$$a = \frac{A_0 Q(G-\rho g)e^{Q/RT_0}}{RT_0^2} \tag{32}$$

and

$$b = A_0 e^{Q/RT_0} \tag{33}$$

such that the solution to equation 28 becomes:

$$u = u_0 - 2b(\rho g \sin\alpha)^3 \int_0^z az'(H-z')^3 dz' \tag{34}$$

Note that the derivation presented above is entirely derived by myself and is likely speculative at best. Non-isothermal models do exist (e.g. [11, 2]). outlining the approaches taken in these studies is, however, beyond the scope of this study.

6 Conclusion

This short case study had the primary purpose to outline the basics computational mechanics behind the numerical solution to a complex diffusive equation, in this case, the shallow ice approximation. In addition, I presented an example of a modular addition to this model. It is clear that the model does not fully encapsulate the physics of glacier flow. Particularly, SIA approximations fail to appropriately describe steeper topographic and velocity gradients [9]; the calving boundary is extremely simplistic and fails to describe complex grounding line dynamics which can either stunt or accelerate glacier flow; SMB forcing is very simplified and does not account for any ablation processes; no basal sliding/sediment deformation mechanisms are taken into account; and, as discussed above, the temperature dependence is not fully described. Based on this model alone it is difficult to assess the relative importance of these processes.

However, as it was set out to be done, the model *does* provide insight on the long term sensitivity to forcing agents. In fact, it has been implemented with success to describe sensitivity to evolving, temperature-driven, fluidity and SMB conditions. In this model I find that temperature may indeed play an important role in the continental scale dynamics of the AIS. Specifically, I find that even with temperature forcing well bellow the current rates, the modelled volume of ice on the AIS can project in radically different conditions depending on the projected temperature trends. In addition, based on this model, under realistic temperature/precipitation correlations, it appears the increased precipitation rate is does not have a, comparatively, significant effect on the long term evolution of the AIS.

Comment

A big time sink in doing this project revolved around the *difusion* function in Buelers code. The issue, here, was that since this code was created, *MatLab* has since included its own built in *diffusion* function which implies that any change made to the Bueler's function was irrelevant because the function was not being queried in the first place-hence the renamed function newdiffusion. Notwithstanding small changes associated to the inclusion of the temperature module, the *diffusion* function (now *newdiffusion*) was otherwise fully functional. The silver lining, as is often the case when debugging, is that I gained intimate familiarity with the functionality of code.

Another note is that the model outputs presented in this study are quite different than those present by Bueler. The reason for this, I believe, is that Bueler did not convert his fluidity, A, into SI units. In the original model, the fluidity is on the order of 10^{-16} but does not indicate units. The values is appropriate is taken in $s^{-1}(kPa)^{-3}$ [12], however to properly integrate with the rest of the model, kilo-pascal units converted to pascal units.

7 Appendix

Link to the original code developed by Bueler:

https://github.com/bueler/karthaus/tree/master/mfiles

Adapted functions are included in in the submission. *ant.m* is the master function it acquires data for the AIS with the *bluidant.m* function, assembles it, and prescribes the variables that will be numerically solved by *siageneral.m* and *newdiffusion.m* over specific time blocks. Smaller time incrementation is then prescribed to the *siageneral.m* function. The *newdiffusion.m* has its own built-in time stepping. Most of the additions made on my part where made in the *ant.m* function. Please feel free to contact me for additional information.

References

[1] Jonathan L Bamber, Riccardo EM Riva, Bert LA Vermeersen, and Anne M LeBrocq. Reassessment of the potential sea-level rise from a collapse of the west antarctic ice sheet. *Science*, 324(5929):901–903, 2009.

[2] Dambaru Raj Baral, Kolumban Hutter, and Ralf Greve. Asymptotic theories of large-scale motion, temperature, and moisture distribution in land-based polythermal ice sheets: a critical review and new developments. *Applied Mechanics Reviews*, 54(3):215–256, 2001.

[3] J. Bohlander and T. Scambos. Thermap antarctic ice sheet temperature data. *National Snow and Ice Data Center. Digital media.*

[4] Katja Frieler, Peter U Clark, Feng He, Christo Buizert, Ronja Reese, Stefan RM Ligtenberg, Michiel R Van Den Broeke, Ricarda Winkelmann, and Anders Levermann. Consistent evidence of increasing antarctic accumulation with warming. *Nature Climate Change*, 5(4):348–352, 2015.

[5] TJ Fudge, Bradley R Markle, Kurt M Cuffey, Christo Buizert, Kendrick C Taylor, Eric J Steig, Edwin D Waddington, Howard Conway, and Michelle Koutnik. Variable relationship between accumulation and temperature in west antarctica for the past 31,000 years. *Geophysical Research Letters*, 43(8):3795–3803, 2016.

[6] Taras Gerya. *Introduction to numerical geodynamic modelling.* Cambridge University Press, 2009.

[7] Rupert M. Gladstone, Victoria Lee, Jonathan Rougier, Antony J. Payne, Hartmut Hellmer, Anne Le Brocq, Andrew Shepherd, Tamsin L. Edwards, Jonathan Gregory, and Stephen L. Cornford. Calibrated prediction of pine island glacier retreat during the 21st and 22nd centuries with a coupled flowline model. *Earth and Planetary Science Letters*, 333–334:191 – 199, 2012.

[8] Philippe Huybrechts. Ice sheet modeling. *in: B. Riffenburgh (ed): Encyclopedia of the Antarctic, Routledge, New York and London*, pages 514–517, 2007.

[9] Emmanuel Le Meur, Olivier Gagliardini, Thomas Zwinger, and Juha Ruokolainen. Glacier flow modelling: a comparison of the shallow ice approximation and the full-stokes solution. *Comptes Rendus Physique*, 5(7):709–722, 2004.

[10] Michael E Mann, Zhihua Zhang, Malcolm K Hughes, Raymond S Bradley, Sonya K Miller, Scott Rutherford, and Fenbiao Ni. Proxy-based reconstructions of hemispheric and global surface temperature variations over the past two millennia. *Proceedings of the National Academy of Sciences*, 105(36):13252–13257, 2008.

[11] LW Morland and GD Smith. Influence of non-uniform temperature distribution on the steady motion of ice sheets. *Journal of Fluid Mechanics*, 140:113–133, 1984.

[12] WSB Paterson. *The physics of glaciers.* Butterworth-Heinemann, 1994.

[13] Isabella Velicogna. Increasing rates of ice mass loss from the greenland and antarctic ice sheets revealed by grace. *Geophysical Research Letters*, 36(19), 2009.